

# The effect of substrate roughness on the surface structure of TiO<sub>2</sub>, SiO<sub>2</sub>, and doped thin films prepared by the sol–gel method

JUSTYNA KRZAK-ROŚ<sup>1</sup>, JAROSŁAW FILIPIAK<sup>2</sup>, CELINA PEZOWICZ<sup>2</sup>,  
AGNIESZKA BASZCZUK<sup>1</sup>, MIROŚLAW MILLER<sup>4,5</sup>, MACIEJ KOWALSKI<sup>3</sup>, ROMUALD BĘDZIŃSKI<sup>2,\*</sup>

<sup>1</sup> Institute of Materials Science and Applied Mechanics, Wrocław University of Technology, Poland.

<sup>2</sup> Institute of Machine Design and Operation, Wrocław University of Technology, Poland.

<sup>3</sup> Institute of Production Engineering and Automation, Wrocław University of Technology, Poland.

<sup>4</sup> Faculty of Chemistry, Wrocław University of Technology, Poland.

<sup>5</sup> EIT+ Wrocław Research Centre, Poland.

Pure and calcium-doped silica and titanium dioxide thin films were prepared by the sol–gel method. Two different metallic substrates, i.e. stainless steel (316L) and titanium alloy (Ti6Al4V), were used for thin film deposition. Physicochemical properties and roughness of the thin films derived were investigated using the Raman spectroscopy, X-ray diffraction analysis, scanning electron microscopy and Taylor–Hobson's surface analyser. It is suggested that the synthesized coatings display physicochemical and surface properties suitable for materials used for implant.

*Key words: thin films, coatings, sol–gel method, roughness*

## 1. Introduction

Contemporary orthopaedics commonly uses various types of implants which replace damaged or malfunctioning parts of the osteoarticular system. The implants are manufactured using a number of construction materials fulfilling specific requirements. To numerous metallic materials belong austenitic steels, Co-Cr alloys, Ni-Cr alloys, and titanium alloys. The materials used for the implants working for a long time in a living organism environment ought to be bioacceptable, resistant to the influence of the tissue environment, and compatible biochemically. Also the implant surfaces are known to be very important, because their chemical, biomechanical, and topographic features influence the behaviour of cells during the initial stage of the implant integration with the sur-

rounding tissues, ultimately determining the speed and the quality of new tissue formation [1], [2].

The development of the interaction between the bone tissue and implant depends on the interaction of the bone matrix and osteoblasts with the biomaterial. Adhesion of the cells and their distribution depend, especially in the first phase after implantation, on the interaction between cells and metallic material and, to a large extent, on the geometric characteristics of the implant surface itself, i.e. its roughness and porosity [3], [4].

Titanium alloys are currently the implant materials most frequently used in various medical applications. These materials most effectively fulfil the expectations and, which is important, enable execution of durable implants, which stay inside a body for more than a dozen or even several dozen years. Despite so many advantageous features exhibited by implants

---

\* Corresponding author: Romuald Będziński, Institute of Machine Design and Operation, Wrocław University of Technology, ul. Łukasiewicza 7/9, 50-371 Wrocław, Poland. E-mail: romulad.bedzinski@pwr.wroc.pl

Received: May 15th, 2009

Accepted for publication: July 25th, 2009

made of titanium alloys, the search for the solutions that could accelerate and improve both development and stability of a bone–implant junction has been continued. This is especially important when we consider the fact that the intensity of growth of bone tissue on the implant surface is connected with the degree of the surface roughness [5], [6]. Physical properties of metallic materials which accelerate the development of bone–implant interactions can be improved by various techniques of surface film engineering, e.g. by the deposition of thin oxide films by the sol–gel method [7]–[10].

The main purpose of the present paper is a physico-chemical characterization of new sol-gel derived TiO<sub>2</sub> and SiO<sub>2</sub> coatings deposited on the surfaces of titanium alloy (Ti6Al4V) and stainless steel (316L). Because the presence of calcium ions has been reported to be advantageous to cell growth [11], calcium-doped TiO<sub>2</sub> and SiO<sub>2</sub> coatings were prepared and analyzed.

Also, the influence of substrate morphology on the final topography of the coatings obtained was investigated.

## 2. Materials and methods

Two different metallic substrates, i.e. stainless steel (316L) and titanium alloy (Ti6Al4V), were used

1.79; TEOS/DEMS mass ratio = 2.5). The titanium precursor used was titanium(IV) isopropoxide (TIPO, Sigma-Aldrich Co.). As indicated by the number of literature citations [12], [13], a correct choice of the precursor used in the process of sol–gel thin film production has a very strong impact on the final properties of the film. The choice of precursors was based on a long experience in obtaining such thin films on different substrates.

Ethanol and isopropanol were used as the solvents. In silica hydrolysates, the reaction catalyst was hydrochloric acid (HCl, POCH S.A.), while in titanium hydrolysates, the stabiliser was acetylacetone (AcAc, Sigma-Aldrich Co.). In order to introduce calcium ions, hydrolysates were doped with the Ca(NO<sub>3</sub>)<sub>2</sub>·4H<sub>2</sub>O (POCH S.A.) solution. The molar ratios of Si/Ca and Ti/Ca were 19.52 and 6.72, respectively. The ingredients were homogenised with a magnetic stirrer for 1–2 hours, depending on the hydrolysate type. The reagents used were purchased from Sigma-Aldrich Co. and from POCH S.A.

Obtained precursors of sols were dip-coated onto the cleaned metallic substrates. Ultimately, four different coatings (pure and calcium-doped silica and titanium dioxide) were deposited obtained on each type of substrate of four different types of roughness (32 samples in total, table 1).

Each film was obtained by dip-coating. The dipping process was conducted 3 times.

Table 1. List of the cases analysed, depending on the type of substrate material, the substrate roughness, and the film applied

Thin film type	Substrate, 316L				Substrate, Ti6Al4V			
	$R_a = 0.16$	$R_a = 0.63$	$R_a = 1.25$	$R_a = 2.50$	$R_a = 0.16$	$R_a = 0.63$	$R_a = 1.25$	$R_a = 2.50$
TiO <sub>2</sub>	✓	✓	✓	✓	✓	✓	✓	✓
TiO <sub>2</sub> + Ca	✓	✓	✓	✓	✓	✓	✓	✓
SiO <sub>2</sub>	✓	✓	✓	✓	✓	✓	✓	✓
SiO <sub>2</sub> + Ca	✓	✓	✓	✓	✓	✓	✓	✓

for thin film deposition. In both cases, the substrates of four different roughness coefficients ( $R_a$ ) with the nominal values of 0.16, 0.63, 1.25, and 2.5  $\mu\text{m}$  were used. The substrates were in the form of cuboidal samples (50 mm  $\times$  10 mm  $\times$  1 mm). Before the deposition of coatings the substrates were washed with acetone, distilled water, and ethyl alcohol.

Inorganic thin films were synthesised using the sol–gel method that is based on the hydrolysis of alkoxide precursors at room temperature. Tetraethoxyorthosilicate (TEOS, Sigma-Aldrich Co.) and diethoxydimethylsilane (DEMS, Sigma-Aldrich Co.) were used as silica precursors (TEOS/DEMS molar ratio =

The speed of dipping and pulling out as well as the immersion time were controlled. The deposited three-layer films were dried at room temperature in air and then annealed for 1 hour at a temperature of 500 °C with a controlled temperature gradient.

The physicochemical tests were carried out using X-ray diffraction and the Raman spectroscopy. The crystal structure of the films was examined by X-ray diffractometer, ULTIMA IV-Rigaku, with thin film attachment, in the  $2\theta$  range of 15–80 degree using CuK $\alpha$  radiation with the wavelength of 0.15406 nm. The Raman study was performed by LabRAM HR800, Horiba Jobin Yvon.

The surface morphology of the samples was analysed with a scanning electron microscope (SEM) HITACHI S-3400N. This allowed the determination of characteristic properties of the  $\text{TiO}_2$  and  $\text{SiO}_2$  films and analogical calcium-doped coatings, which are present irrespective of the type of the substrate used.

The tests of a 2D surface roughness were carried out in accordance with PN-EN ISO 4288:1999 [14] on the Form Talysurf 120L surface analyser by Taylor Hobson. Measurements were carried out by the tracer method, using a conical gauging point made of a diamond with the tip roundness radius of 2  $\mu\text{m}$  and the tip angle of 90°. In accordance with the Polish standard PN-EN ISO 3274:1997, the adopted measuring length  $l_n$  was equal to 8 mm, which during the analysis of measured profiles and the calculations of roughness parameters was divided into sampling lengths  $l_r = 0.8$  mm. The measured profile presents total effects of roughness, waviness, and shape errors. To separate those irregularities and to select from them the part of the signal considered to be roughness, a Gaussian highpass filter was used (attenuating lower frequency signals, i.e. waviness and shape errors) with the limit wavelength  $\lambda_c = 0.8$ .

### 3. Results

#### 3.1. X-ray diffraction measurements

Thin films deposited on the surface of the both types of substrates (316L and Ti6Al4V) were examined after their drying at room temperature and after annealing at 500 °C in the air (1 h). The analysis of X-ray diffraction patterns measured for both pure  $\text{SiO}_2$ ,  $\text{TiO}_2$  and doped films showed that all the samples before heating were amorphous.

Pure and  $\text{Ca}^{2+}$ -doped silica coatings remained amorphous after annealing at 500 °C. Figure 1 presents the examples of the patterns obtained for those films on titanium alloy substrates. The only visible peaks arise from the substrate – Ti6Al4V.

A direct comparison of X-ray diffraction patterns of the pure  $\text{TiO}_2$  films with  $\text{Ca}^{2+}$ -doped  $\text{TiO}_2$  films shows an interesting difference in their crystalline structure. Pure  $\text{TiO}_2$  films have an anatase structure (very intensive peaks at  $2\theta \approx 25^\circ$ ). By contrast,  $\text{Ca}^{2+}$ -doped  $\text{TiO}_2$  films, apart from the bands from anatase, display visible characteristic peak from brookite (at  $2\theta = 31^\circ$ ). Figure 2 shows X-ray diffraction pat-

terns of the pure  $\text{TiO}_2$  film and  $\text{Ca}^{2+}$ -doped  $\text{TiO}_2$  film with the patterns of anatase and brookite from ICSD database for comparison.

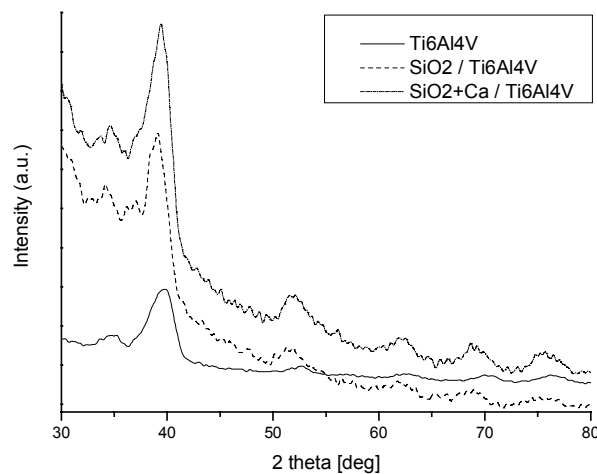


Fig. 1. X-ray diffraction patterns of the pure and doped  $\text{SiO}_2$  films. X-ray diffraction pattern measured on metallic substrate (solid line) is shown for comparison

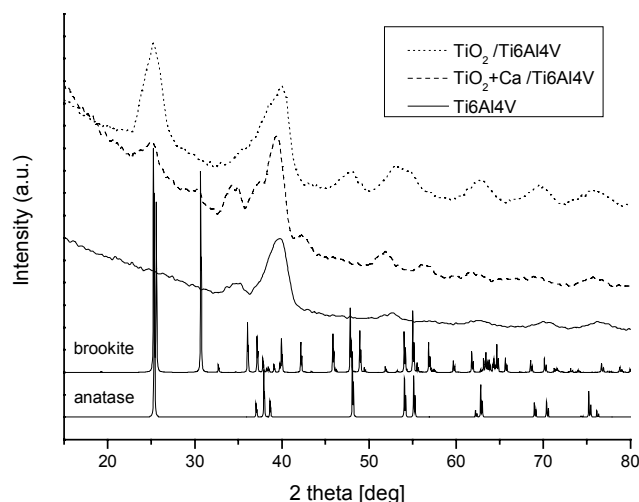


Fig. 2. X-ray diffraction patterns of the pure and calcium-doped  $\text{TiO}_2$ . X-ray diffraction pattern measured on metallic substrate (solid line) is shown for comparison

#### 3.2. Raman spectra analysis

Based on the analysis of the Raman spectra it was found that pure titanium dioxide coatings contained  $\text{TiO}_2$  only in the anatase form. The analysis of fundamental vibrations typical of anatase showed six active vibrations in the Raman spectra:  $A_{1g} + 2B_{1g} + 3E_g$ . They are characteristic of tetragonal anatase phase which corroborates previous reports [15], [16].

The bands representing those vibrations were observed in the spectra measured for pure  $\text{TiO}_2$  films at the

frequencies of  $149\text{ cm}^{-1}$ ( $E_g$ ),  $195\text{ cm}^{-1}$ ( $E_g$ ),  $396\text{ cm}^{-1}$ ( $B_{1g}$ ),  $513\text{ cm}^{-1}$ ( $A_{1g}$ ), and  $637\text{ cm}^{-1}$ ( $E_g$ ).

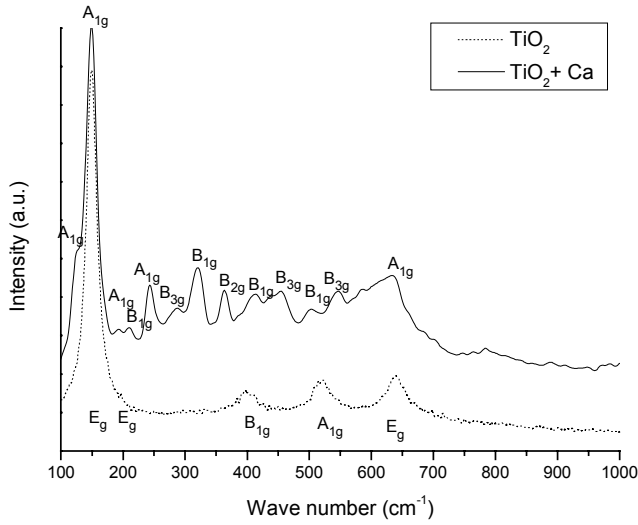


Fig. 3. Raman spectra of the  $\text{TiO}_2$  and  $\text{Ca}^{2+}$ -doped  $\text{TiO}_2$  films on the Ti6Al4V substrate

The Raman spectra measured for  $\text{Ca}^{2+}$ -doped  $\text{TiO}_2$  films are different from these recorded for pure  $\text{TiO}_2$  films. They display additional bands coming from brookite – the metastable crystalline form of  $\text{TiO}_2$  [17]–[19]. Table 2 shows the bands typical of brookite observed for  $\text{Ca}^{2+}$ -doped  $\text{TiO}_2$  films.

Table 2. Characteristic vibrations of crystalline brookite form and corresponding bands observed for  $\text{Ca}^{2+}$ -doped  $\text{TiO}_2$  films

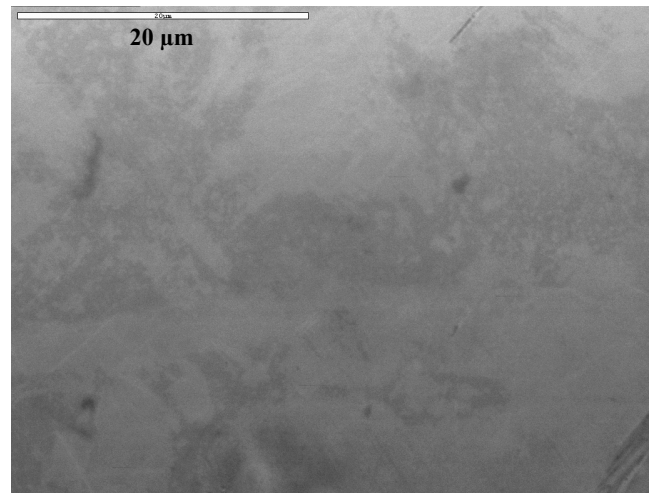
No.	Characteristic vibrations	Wave frequency ( $\text{cm}^{-1}$ )
1	$A_{1g}$	123, 150, 191, 243, 635
3	$B_{1g}$	212, 321, 412, 500
6	$B_{2g}$	363, 584
8	$B_{3g}$	290, 453, 548

Slight differences compared with data reported in [15]–[19] are reasonable due to the structural distortions in the thin film or intragranular defects in samples.

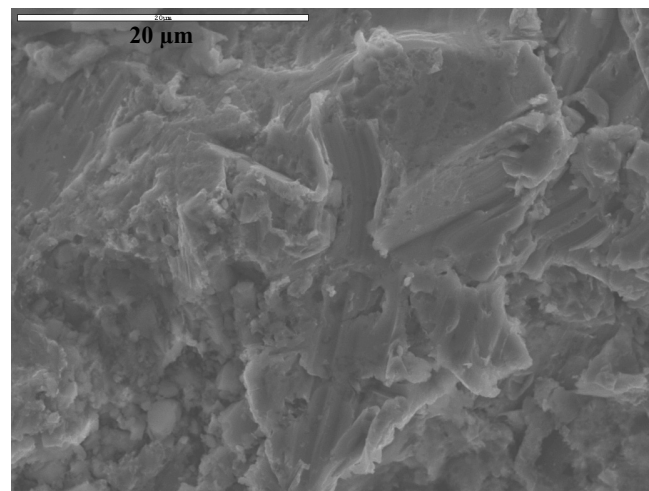
Based on the analysis of the Raman spectra representing pure and  $\text{Ca}^{2+}$ -doped silica dioxide it was concluded that the bands observed come from vibrations characteristic of the amorphous  $\text{SiO}_2$  ( $493\text{ cm}^{-1}$ ,  $601\text{ cm}^{-1}$ ,  $800\text{ cm}^{-1}$ ,  $967\text{ cm}^{-1}$ ,  $1276\text{ cm}^{-1}$ ,  $1410\text{ cm}^{-1}$ ). Additionally the coatings also contained the remains of organic substances. At the frequencies of  $2807\text{ cm}^{-1}$ ,  $2914\text{ cm}^{-1}$ ,  $2975\text{ cm}^{-1}$ , and  $3596\text{ cm}^{-1}$  bands coming from the vibrations of  $\text{CH}_3$  organic groups were observed.

### 3.3. SEM examinations

Microscopic examinations (SEM) showed that coatings applied on the substrates with low-roughness ( $R_a = 0.16$ ,  $R_a = 0.63$ ) had a continuous surface with a mesh of tiny elongated pits (figures 4–9). If the roughness of substrates was higher ( $R_a = 1.25$  and  $R_a = 2.5$ ), characteristic cracking appeared on the coating surface. SEM analysis showed the cracks within the second and third layers of the film. The first layer, i.e. the one in direct contact with the substrate, was continuous. Table 3 shows gap width ranges measured for  $\text{TiO}_2$  and  $\text{SiO}_2$  coatings deposited on the substrates with different roughness.



a)



b)

Fig. 4. SEM images of 316L steel substrates without the film, two extreme roughness values of substrates (3000× magnification): a)  $R_a = 0.16\text{ }\mu\text{m}$ ; b)  $R_a = 2.5\text{ }\mu\text{m}$

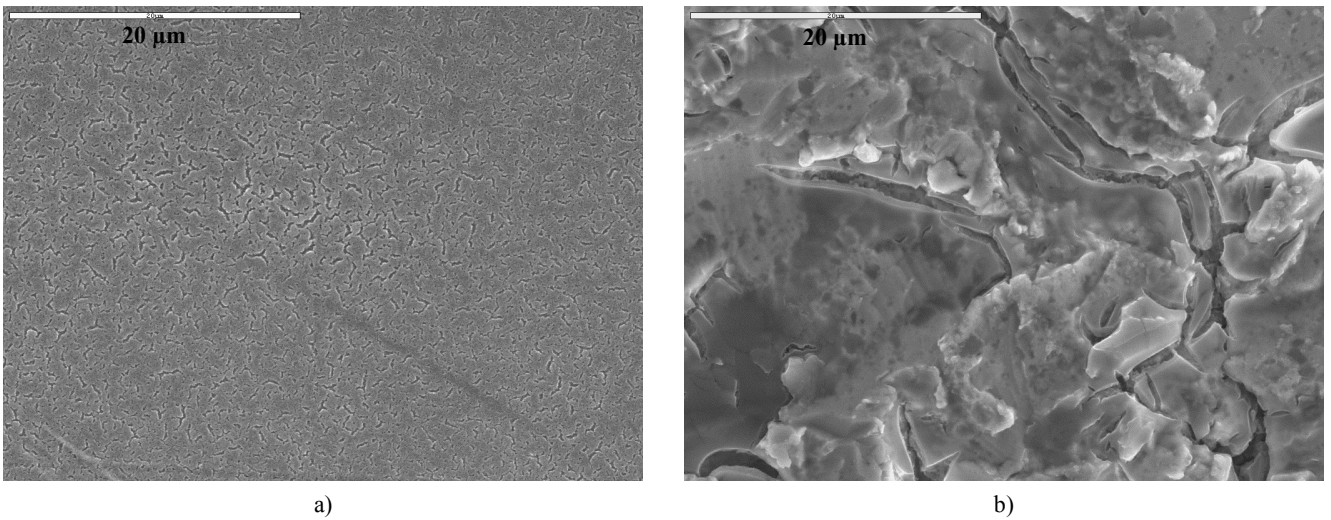


Fig. 5. SEM images of  $\text{TiO}_2$  coatings on 316L steel, two extreme roughness values of substrates (3000 $\times$  magnification):  
a)  $R_a = 0.16 \mu\text{m}$ ; b)  $R_a = 2.5 \mu\text{m}$

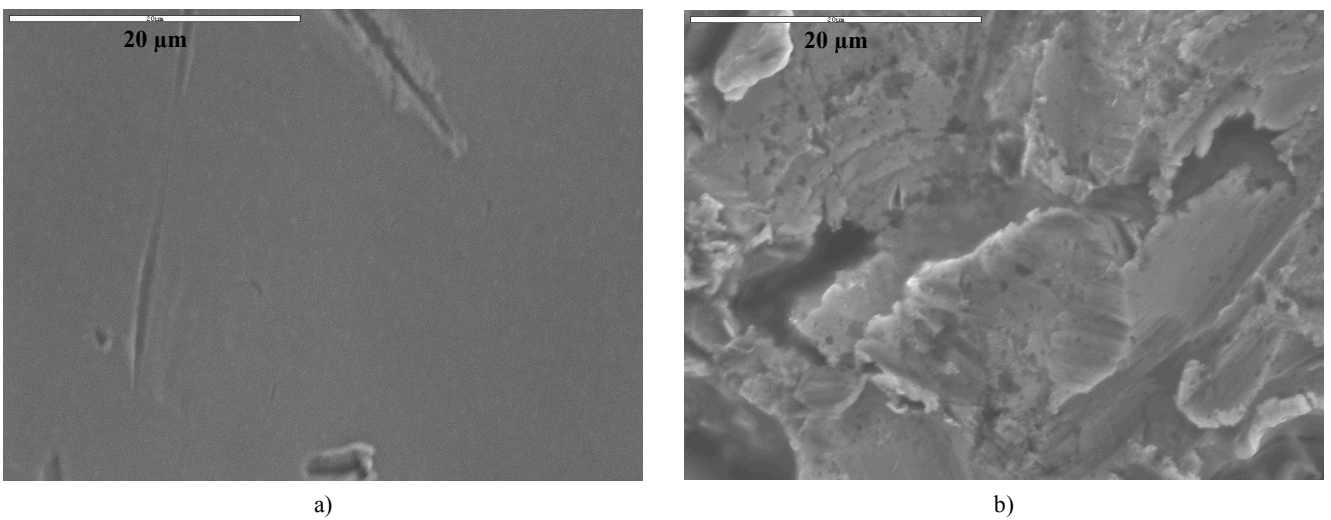


Fig. 6. SEM images of  $\text{SiO}_2$  coatings on 316L steel, two extreme roughness values of substrates (3000 $\times$  magnification):  
a)  $R_a = 0.16 \mu\text{m}$ ; b)  $R_a = 2.5 \mu\text{m}$

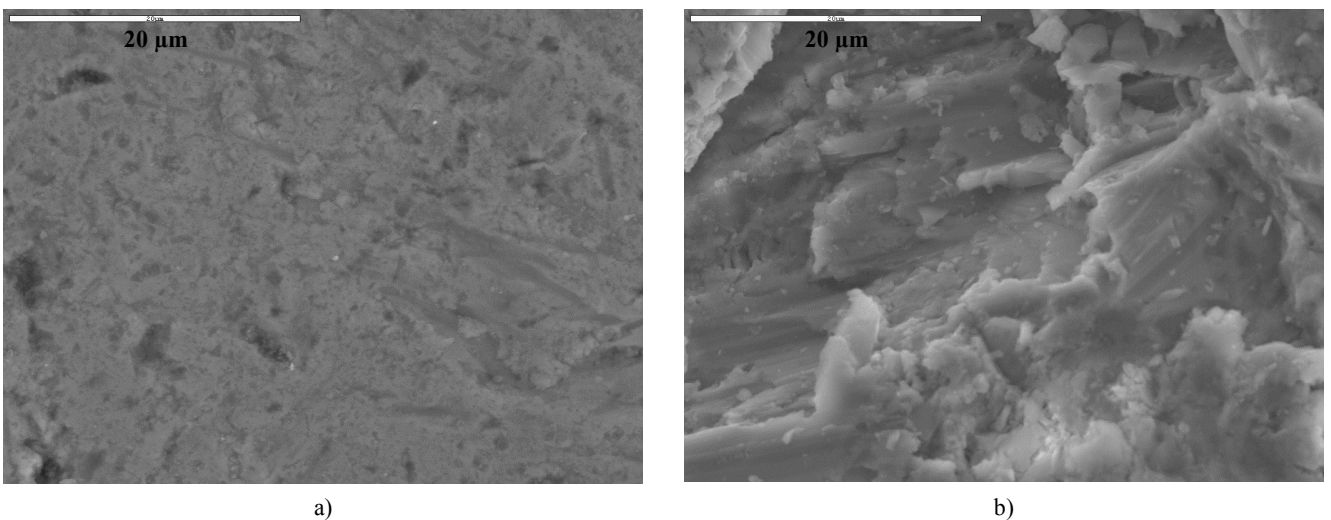


Fig. 7. SEM images of Ti6Al4V substrates without the film; two extreme roughness values of substrates (3000 $\times$  magnification):  
a)  $R_a = 0.16 \mu\text{m}$ ; b)  $R_a = 2.5 \mu\text{m}$

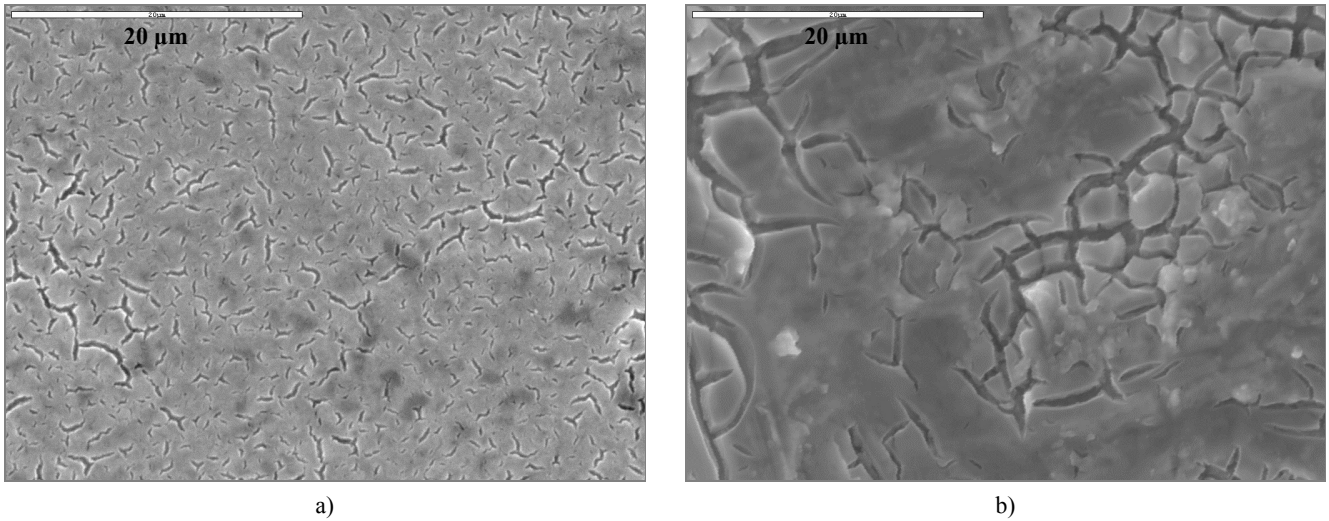


Fig. 8. SEM images of TiO<sub>2</sub> coatings on Ti6Al4V, two extreme roughness values of substrates (3000× magnification):  
 a)  $R_a = 0.16 \mu\text{m}$ ; b)  $R_a = 2.5 \mu\text{m}$

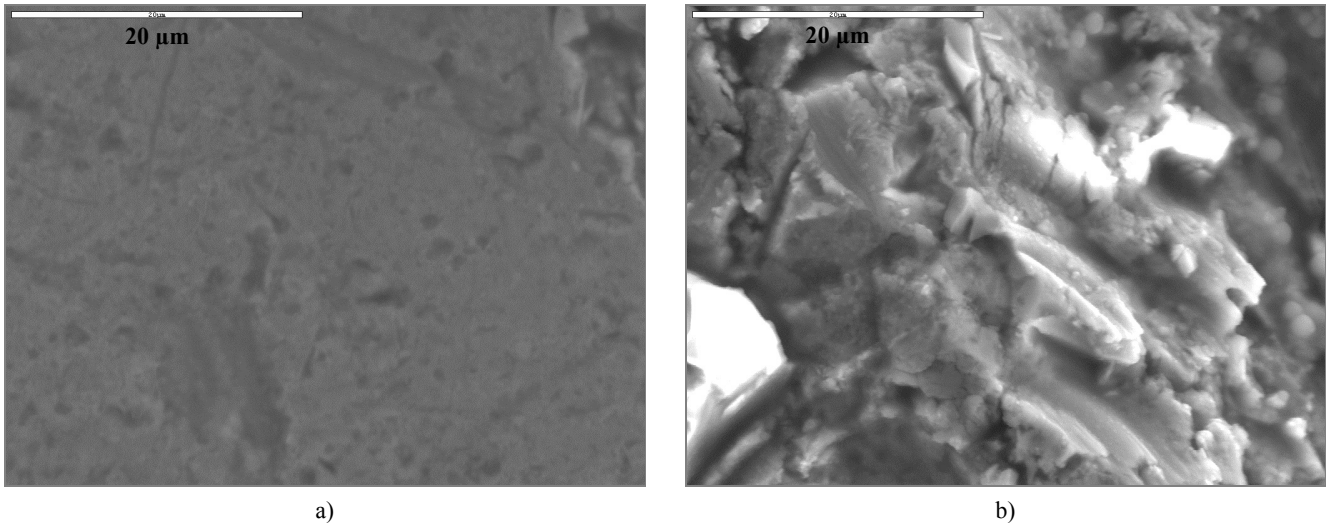


Fig. 9. SEM images of SiO<sub>2</sub> coatings on Ti6Al4V, two extreme roughness values of substrates (3000× magnification):  
 a)  $R_a = 0.16 \mu\text{m}$ ; b)  $R_a = 2.5 \mu\text{m}$

Table 3. Gap width ranges in the TiO<sub>2</sub> and SiO<sub>2</sub> films, depending on the substrate nominal roughness  $R_a$  (in  $\mu\text{m}$ )

Films	$R_a = 0.16$	$R_a = 0.63$	$R_a = 1.25$	$R_a = 2.5$
Ti6Al4V+TiO <sub>2</sub>	0.18÷0.45	0.21÷0.45	0.52÷1.26	0.56÷1.72
Ti6Al4V+SiO <sub>2</sub>	0.62÷1.05	1.15÷1.41	1.45÷3.00	1.68÷3.20
316L+TiO <sub>2</sub>	0.11÷0.35	0.28÷0.58	0.64÷1.55	0.74÷1.90
316L+SiO <sub>2</sub>	0.45÷0.85	1.12÷1.83	1.40÷3.45	2.11÷3.66

Analyzing the gap width ranges obtained for TiO<sub>2</sub> and SiO<sub>2</sub> films it is clear that SiO<sub>2</sub> films always demonstrate much broadened gaps, irrespective of the substrate type (Ti6Al4V, 316L) and its roughness.

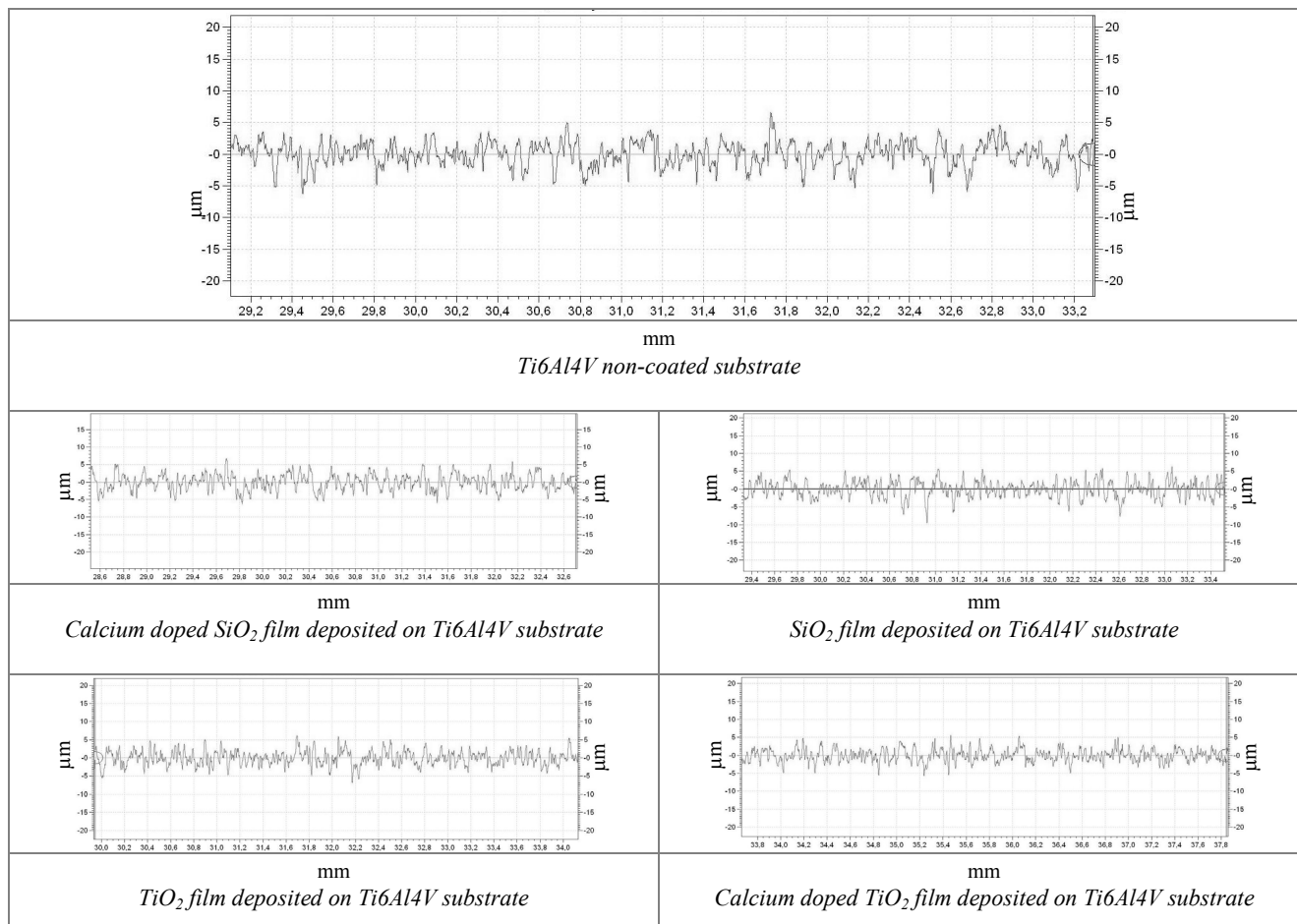
### 3.4. Roughness

During the first stage of the research the surface roughness parameters for 316L stainless steel and

Ti6Al4V titanium alloy substrates without coatings were measured and determined [20], [21]. In the second stage, the surface roughness tests were carried out after SiO<sub>2</sub>, TiO<sub>2</sub>, SiO<sub>2</sub>+Ca, and TiO<sub>2</sub>+Ca thin film deposition. Each measurement was repeated three times and the parameter values were subjected to analysis, constituting an average of the three measurements. Table 4 presents the examples of roughness measurements carried out on Ti6Al4V samples.

different types of roughness with the nominal values:  $R_a = 0.16 \mu\text{m}$ ,  $R_a = 0.63 \mu\text{m}$ ,  $R_a = 1.25 \mu\text{m}$ , and  $R_a = 2.5 \mu\text{m}$ , the changes of the parameters from all four groups are within the limits of a measuring error due to the application of the tracer method of surface scanning. The directionless point structure, prepared for the application of films, was also characterised by the largest heterogeneity, and the measuring accuracy in the case of such a structure was  $\pm 30\%$ . Obviously,

Table 4. Examples of roughness measurements of 2D profiles of Ti6Al4V sample



In the latest released measurement software, Taylor-Hobson has proposed a division of the 2D roughness parameters into 4 groups:

- amplitude-based:  $R_a$ ,  $R_q$ ,  $R_p$ ,  $R_v$ ,  $R_z$ ,  $R_t$ ,  $R_{sk}$ ,  $R_{ku}$ ,  $R_c$ ,  $R_z$ (JIS),  $R_z$ (DIN),  $R_{3z}$ , and  $R_{3y}$ ,
- hybrid:  $R_{Aq}$ ,  $R_{Aq}$ ,  $R_{Aa}$ , and  $R_{Vo}$ ,
- length-based:  $R_{Sm}$ ,  $R_{HSC}$ ,  $R_{Pc}$ ,  $R_{Lo}$ ,  $R_S$ , and  $R_{In}$ ,
- read out from the bearing area curve:  $R_{\delta c}$ ,  $R_{mr}$ , and  $R_{mr}(C)$ .

Based on the analysis of the above-mentioned parameters it was concluded that for all the samples made of the 316L steel and Ti6Al4V alloy of four

due to the large surface spread and good adhesion it is often used to apply coatings; however, obtaining a nominal, target output roughness is complicated and subject to a serious error.

The comparison of the surface roughness obtained for non-coated clean substrates with that of the substrates with coatings showed that the surface films changed the substrate roughness properties. In the case of the substrate with the lowest roughness in the group tested ( $R_a = 0.16$ ), after applying SiO<sub>2</sub> and TiO<sub>2</sub> films we observed an increase in its roughness by 8.2% and by over 9%, respectively. Similar results

for low roughness values are presented in the paper [22]. A completely different tendency is observed for substrates of higher roughness. Materials with  $R_a = 0.63$ ,  $R_a = 1.25$  and  $R_a = 2.5$  indicate decrease in the roughness of surfaces after thin films deposition, by more than a dozen percent in the case of the  $\text{SiO}_2$  film and by over 20% in the case of the  $\text{TiO}_2$  film [23]. Similar relationships were recorded both for 316L steel and Ti6Al4V alloy substrates coated with thin films of oxides.

## 4. Discussion and conclusions

As a result of the research conducted, chemically stable silica ( $\text{SiO}_2$ ), titania ( $\text{TiO}_2$ ), and calcium-doped silica/titania coatings were synthesised.

Physicochemical properties and the surface topography of thin films deposited on implant metallic substrates were examined. The results obtained and those previously described [23] provided complete information on the structure of the produced materials.

Physicochemical research based on the results of the Raman spectroscopy and X-ray diffraction proved that before thermal treatment all synthesised materials contained an amorphous phase only. Both pure and doped silica coatings remain amorphous after thermal treatment. Pure  $\text{TiO}_2$  coatings after thermal treatment are transformed into the crystalline form – anatase. X-ray diffraction patterns of  $\text{Ca}^{2+}$ -doped  $\text{TiO}_2$  coatings showed peaks corresponding to an metastable phase of the titanium dioxide – brookite. However, the main peak (101) representing anatase at  $2\theta = 25.5^\circ$  and the peaks representing brookite (121), (111) at  $25.3^\circ$  and  $25.7^\circ$ , respectively, overlap. In order to confirm the validity of the results of X-ray diffraction measurements, the Raman spectra of the materials described were measured.

An analysis of Raman spectra of the calcium-doped  $\text{TiO}_2$  films clearly showed that besides the anatase bands there are some bands belonging to brookite. As is well known, the crystal structure of  $\text{TiO}_2$  films depends on the process condition and the materials used in this process [24]. The Raman bands of anatase and brookite phases observed in the Raman spectra of the samples are broadened compared with bands that can be found in the literature [15], most probably due to the nanocrystalline size of the particles. In any case, a Raman band at  $612\text{ cm}^{-1}$ , typical of the rutile  $\text{TiO}_2$  phase [15], is not observed in the Raman spectra, not even as a shoulder of the band centered at  $638\text{ cm}^{-1}$ . This behaviour is in agreement

with the X-ray analysis which confirms that the titanium oxide thin films are in pure anatase form and  $\text{Ca}^{2+}$ -doped titanium oxide films are the mixture of anatase and brookite.

The tests of surface roughness enabled determining the coating impact on changes of sample roughness. In the case of the substrates with lower roughness ( $0.16\text{ }\mu\text{m}$ ), their roughness increased by several per cent, which corresponds to the results presented in the paper [22]. On the other hand, the substrates with higher roughness ( $0.63$ ,  $1.25$ , and  $2.5\text{ }\mu\text{m}$ ) showed a completely different behaviour. In those cases, after applying a three-layer coating, there was a drop in the original roughness up to several dozen per cent. Such changes can have a significant importance during biological analyses with the use of cell cultures, therefore it should be remembered that after the application of multi-layered coatings the scope of roughness changes completely. As was demonstrated by research [3], [5], [22], [25], surface roughness of the substrates used for implants has a major influence on the rate of growth of bone tissue and its biological quality.

Microscopic examinations (SEM) revealed characteristic fissures (gaps) on the surface of the film applied onto substrates of higher roughness ( $R_a = 1.25$  and  $R_a = 2.5$ ). In particular, those fissures are present within the second and third layer (the first layer in direct contact with the substrate is continuous). The observed cracking is a result of, among others, contractile tensions appearing in the drying film of hydrolysate coating the surface unevenness. It can be assumed that the presence of such gaps on the implant surface may have a positive effect on implant and tissue biointegration. For example, osteoblasts (bone-forming cells) ‘do not notice’ the gaps smaller than  $0.6\text{ }\mu\text{m}$  [3], [11], which means that on the surface with numerous gaps wider than  $0.6\text{ }\mu\text{m}$ , osteoblasts will readily settle down, proliferate, and synthesise proteins which constitute an origin of bone tissue. This condition settled for gap width on the thin film surfaces is fulfilled for thin  $\text{SiO}_2$  films deposited on Ti6Al4V and on 316L steel whose roughness is in the whole measuring range. It seems that  $\text{TiO}_2$  films of higher roughness ( $R_a = 1.25$  and  $2.5$ ) also fulfil this condition and can be considered to be the promising coating of durable implants.

The results of the tests show that by matching the substrate roughness to the sol-gel oxide coatings it is possible to make the topography of the implant surface different. Depending on the assumed purpose of the treatment, the surfaces obtained could be appropriate for the implants of either short-term or long-term durability. In the case of the implants of long-



term durability, the surface obtained in the experiment (roughness + coating) would ensure good implant biointegration with the bone tissue (a higher value of the roughness coefficient ( $R_a$ )). Additionally, irrespective of the metallic material surface topography, the oxide coatings have a positive impact on biocompatibility by separating the metallic material from the tissue environment.

### Acknowledgements

This work was supported by the research grants N507 009 31/0275 and N N507 4491 33 from the Polish Ministry of Science and Higher Education.

### Literature

- [1] BOWERS K.T., KELLER J.C., RANDOLPH B.A., WICK D.G., MICHAELS C.M., *Optimization of surface micromorphology for enhanced osteoblast responses in vitro*, Int. J. Oral Maxillofac. Implants, 1992, 7(3), 302–310.
- [2] BRUNETTE D.M., *The effects of implant surface topography on the behaviour of cells*, Int. J. Oral Maxillofac. Implants, 1988, 3, 231–246.
- [3] ANSELME K., BIGERELLE M., NOEL B., DUFRESNE E., JUDAS D., IOST A., HARDOUIN P., *Qualitative and quantitative study of human osteoblast adhesion on materials with various surface roughnesses*, J. Biomed. Mater. Res., 2000, 49, 155–66.
- [4] KONONEN M., HORNIA M., KIVILAHTI J., HAUTANIEMI J., THESLEFF I., *Effect of surface processing on the attachment, orientation, and proliferation of human gingival fibroblasts on titanium*, J. Biomed. Mater. Res., 1992, 26, 1325–1341.
- [5] MURRAY D.W., RAE T., RUSHTON N., *The influence of the surface energy and roughness of implants on bone resorption*, JBJS (Br), 1989, 71-B (4), 632–637.
- [6] SATSANGI A., SATSANGI N., GLOVER R., SATSANGI R.K., ONG J.L., *Osteoblast response to phospholipid modified titanium surface*, Biomaterials, 2003, 24, 4585–4589.
- [7] GLUSZEK J., *Tlenkowe powłoki ochronne otrzymywane metodą sol-gel*, Wrocław, 1998.
- [8] KRZAK-ROŚ J., GRYGIER D., BASZCZUK A., BĘDZIŃSKI R., *Mechanical and physico-chemical properties of titanium dioxide thin films*, Engineering of Biomaterials, 2007, X(67-68), 35–37.
- [9] OCHSENBEIN A., CHAI F., WINTER S., TRASNEL M., BREME J., HILDEBRAND H.F., *Osteoblast responses to different oxide coatings produced by the sol-gel process on titanium substrates*, Acta Biomaterialia, 2008, 4, 1506–1517.
- [10] GRYGIER D., DUDZIŃSKI W., WIKTORCZYK T., HAIMANN K., *Effect of silica precursors-type on mechanical properties of sol-gel coatings*, Acta Bioeng. Biomech., 2008, 10(1), 27–35.
- [11] ZHU X., CHEN J., SCHEIDELER L., REICHL R., GEIS-GERSTORFER J., *Effects of topography and composition of titanium surface oxides on osteoblast responses*, Biomaterials, 2004, 25, 4087–4103.
- [12] FALARAS P., XAGAS A.P., *Roughness and fractality of nanostructured TiO<sub>2</sub> films prepared via sol-gel techniques*, J. Mat. Science, 2002, 37, 3855–3860.
- [13] TING C.C., CHEN S.Y., *Influence of ligand groups in Ti precursors on phase transformation and microstructural evolution of TiO<sub>2</sub> thin films prepared by the wet chemical process*, J. Mater. Res., 2001, 16 (6), 1712–1719.
- [14] PN-ISO 4288: 1997 + Ap1: 1999, *Wymagania geometryczne wyrobów. Struktura geometryczna powierzchni. Zasady i procedury oceny struktury geometrycznej powierzchni metodą profilową*.
- [15] OHSAKA T., IZUMI F., FUJIKI Y., *Raman spectrum of anatase, TiO<sub>2</sub>*, J. Raman Spectrosc., 1978, 7, 321–324.
- [16] WANG Z., SAXENA S.K., *Raman spectroscopic study on pressure-induced amorphization in nanocrystalline anatase (TiO<sub>2</sub>)*, Solid State Communications, 2001, 118, 75–78.
- [17] TOMPSETT G.A., BOWMAKER G.A., COONEY R.P., METSON J.B., RODGERS K.A., SEAKINS J.M., *The Raman spectrum of brookite, TiO<sub>2</sub> (Pbca, Z = 8)*, J. Raman Spectrosc., 1995, 26(1), 57–62.
- [18] HU Y., TAI H.L., HUANG C.L., *Effect of brookite phase on the anatase-rutile transition in titania nanoparticles*, J. European Ceramic Society, 2003, 23, 691–696.
- [19] DJAOUED Y., BRUNING R., BERSANI D., LOTTICI P.P., BADILESCU S., *Sol-gel nanocrystalline brookite-rich titania films*, Materials Letters, 2004, 58, 2618–2622.
- [20] NOWICKI B., *Struktura geometryczna. Chropowatość i falistość powierzchni*, WNT, Warszawa, 1991.
- [21] ŻEBROWSKI H., KOWALSKI M., *Pomiary i analiza stereometryczna (3D) powierzchni po obróbce strumieniowo-ściernej. Zagadnienia inżynierii powierzchni w obróbce skrawaniem*, Inżynieria powierzchni, 1999.
- [22] DELIGIANNI D.D., KATSALA N., LADAS S., SOTIROPOULOU D., AMEDEE J., MISSIRLIS Y.F., *Effect of surface roughness of the titanium alloy Ti6Al4V on human bone marrowcell response and on protein adsorption*, Biomaterials, 2001, 22, 1241–1251.
- [23] BĘDZIŃSKI R., FILIPIAK J., PEZOWICZ C., KRZAK-ROŚ J., KOWALSKI M., *Influence of substrate roughness on TiO<sub>2</sub> and SiO<sub>2</sub> coating topography produced by the sol-gel process*, Engineering of Biomaterials, 2008, 11 (81–84), 87–89.
- [24] MECHIAKH R., MERICHE F., KREMER R., BENSABA R., BOUDINE B., BOUDRIOUA A., *TiO<sub>2</sub> thin films prepared by sol-gel method for waveguiding application: Correlation between the structural and optical properties*, Optical Materials, 2007, (30), 645–651.
- [25] TRISI P., RAO W., REBAUDI A., *A histometric comparison of smooth and rough titanium implants in human low-density jawbone*, Int. J. Oral Maxillofac. Implants., 1999, 14(5), 689–698.